УДК 539.171.115

MEASUREMENTS OF THE TOTAL CROSS SECTION DIFFERENCE $\Delta\sigma_L(np)$ AT 1.59, 1.79, AND 2.20 GeV

V.I.Sharov[1], *S.A.Zaporozhets*[1], *B.P.Adiasevich*[2] , *N.G.Anischenko*[1], *V.G.Antonenko*[2], *L.S.Azhgirey*[3], *V.D.Bartenev*[1], *N.A.Bazhanov*[4], *N.A.Blinov*[1], *N.S.Borisov*[3], *S.B.Borzakov*[5], *Yu.T.Borzunov*[1], *L.V.Budkin*[3], *V.F.Burinov*[3], *Yu.P.Bushuev*[1], *L.P.Chernenko*[5], *E.V.Chernykh*[1], *S.A. Dolgii*[1], *V.M.Drobin*[1], *G.Durand*,[6] *A.P.Dzyubak*[7], *A.N.Fedorov*[8], *V.V.Fimushkin*[1], *M.Finger*[3,9], *M.Finger,Jr.*[3], *L.B.Golovanov*[1], *G.M.Gurevich*[10], *A.Janata*[3,11], *A.V.Karpunin*[1], *B.A.Khachaturov*[3], *A.D.Kirillov*[1], *A.D.Kovalenko*[1], *A.I.Kovalev*[4], *V.G.Kolomiets*[3], *A.A.Kochetkov*[12], *E.S.Kuzmin*[3], *V.P.Ladygin*[1], *A.B.Lazarev*[3], *F.Lehar*[6], *A. de Lesquen*[6], *A.A.Lukhanin*[7], *P.K.Maniakov*[1], *V.N.Matafonov*[3], *A.B.Neganov*[3], *M.S.Nikitina*[12], *G.P.Nikolaevsky*[1], *A.A.Nomofilov*[1], *Tz.Panteleev*[5,13], *Yu.K.Pilipenko*[1], *I.L.Pisarev*[3], *N.M.Piskunov*[1], *Yu.A.Plis*[3], *Yu.P.Polunin*[2], *A.N.Prokofiev*[4], *P.A.Rukoyatkin*[1], *O.N.Shchevelev*[3], *V.A.Shchedrov*[4],*S.N.Shilov*[3], *Yu.A.Shishov*[1], *V.B.Shutov*[1], *M.Slunečka*[3,9], *V.Slunečková*[3], *A.Yu.Starikov*[1], *G.D.Stoletov*[3], *L.N.Strunov*[1], *A.L.Svetov*[1], *A.P.Tsvinev*[1], *Yu.A.Usov*[3], *V.I.Volkov*[1], *V.P.Yershov*[1], *A.A.Zhdanov*[4], *V.N.Zhmyrov*[3]

New results for the np spin-dependent total cross section difference $\Delta\sigma_L(np)$ at neutron beam kinetic energies of 1.59, 1.79, and 2.20 GeV are presented. Measurements of the $\Delta\sigma_L(np)$ energy dependence were carried out at the Synchrophasotron of the

[1]Laboratory of High Energies, JINR, 141980 Dubna, Moscow region, Russia.
[2]Scientific Centre "Kurchatov Institute", 123182 Moscow, Russia.
[3]Laboratory of Nuclear Problems, JINR, 141980 Dubna, Moscow region, Russia.
[4]Petersburg Nuclear Physics Institute, High Energy Physics Division, 188350 Gatchina, Russia.
[5]Frank Laboratory of Neutron Physics, JINR, 141980 Dubna, Moscow region, Russia.
[6]DAPNIA, CEA/Saclay, 91191 Gif-sur-Yvette Cedex, France.
[7]Kharkov Institute of Physics and Technology, 310108 Kharkov, Ukraine.
[8]Laboratory of Particle Physics, JINR, 141980 Dubna, Moscow region, Russia.
[9]Charles University, Faculty of Mathematics and Physics, V Holešovičkách 2, 18000 Praha 8, Czech Republic.
[10]Russian Academy of Sciences, Institute for Nuclear Research, 117312 Moscow, Russia.
[11]Academy of Sciences of the Czech Republic, Nuclear Research Institute, 25068 Řež, Czech Republic.
[12]Moscow State University, Faculty of Physics, 119899 Moscow, Russia.
[13]Bulgarian Academy of Sciences, Institute for Nuclear Research and Nuclear Energy, Tsarigradsko shaussee boulevard 72, 1784 Sofia, Bulgaria

Laboratory of High Energies of the Joint Institute for Nuclear Research in Dubna. A quasi-monochromatic neutron beam was produced by break-up of accelerated and extracted polarized deuterons. The neutrons were transmitted through a large proton polarized target. The values of $\Delta\sigma_L$ were measured as a difference between the np total cross sections for parallel and antiparallel beam and target polarizations, both oriented along the beam momentum. The results at the two higher energies were obtained using four combinations of two opposite polarization directions for both the beam and the target. Only one target polarization direction was available at 1.59 GeV. A fast decrease of $\Delta\sigma_L(np)$ with increasing energy above 1.1 GeV, as it was first seen from our previous data, was confirmed. The new results are also compared with model predictions and with the phase shift analysis fits. The $\Delta\sigma_L$ quantities for isosinglet state I=0, deduced from the measured values of $\Delta\sigma_L(np)$ and known $\Delta\sigma_L(pp)$ data, are given.

The investigation has been performed at the Laboratory of High Energies, JINR.

Измерения разности полных сечений $\Delta\sigma_L(np)$ при 1,59, 1,79 и 2,20 ГэВ

В.И.Шаров и др.

Представлены новые результаты по спин-зависимой разности полных np-сечений $\Delta\sigma_L(np)$ при кинетических энергиях пучка нейтронов 1,59, 1,79 и 2,20 ГэВ. Измерения энергетической зависимости $\Delta\sigma_L(np)$ выполнены на синхрофазотроне Лаборатории высоких энергий ОИЯИ. Квазимонохроматический пучок нейтронов создавался путем развала ускоренных и выведенных поляризованных дейтронов. Измерялось пропускание нейтронного пучка большой поляризованной протонной мишенью. Значения $\Delta\sigma_L$ определялись как разность полных np-сечений для параллельно и антипараллельно направленных поляризаций пучка и мишени, ориентированных вдоль направления импульса пучка. Результаты при двух высших энергиях были получены при использовании всех четырех комбинаций направлений поляризаций пучка и мишени. При энергии 1,59 ГэВ измерения выполнены только с одним направлением поляризации мишени. Подтверждено быстрое падение $\Delta\sigma_L(np)$ с ростом энергии выше 1,1 ГэВ, замеченное впервые по нашим предыдущим результатам. Новые данные сравниваются с предсказанием теоретических моделей и с последними решениями фазового анализа. Представлены также значения $\Delta\sigma_L$ для изосинглетного $I = 0$ np-состояния, полученные из измеренных величин $\Delta\sigma_L(np)$ и известных $\Delta\sigma_L(pp)$ данных.

Работа выполнена в Лаборатории высоких энергий ОИЯИ

Dedicated to the 275th anniversary of the Russian Academy of Sciences.

1. INTRODUCTION

This paper presents new results for the spin-dependent neutron-proton total cross section difference $\Delta\sigma_L(np)$ obtained in 1997 with a quasi-monochromatic polarized neutron beam and a polarized proton target (PPT). The values of $\Delta\sigma_L(np)$ were measured at neutron beam kinetic energies of 1.59, 1.79, and 2.20 GeV.

The free polarized neutron beam was produced by break-up of polarized deuterons accelerated and extracted at the Synchrophasotron of the Laboratory of High Energies (LHE) of the Joint Institute for Nuclear Research (JINR) in Dubna. This accelerator provides the highest energy polarized neutron beam, which can be reached now (3.7 GeV).

The spin-dependent observables $\Delta\sigma_L(np)$ and $\Delta\sigma_T(np)$ are defined as a difference in the np total cross sections for antiparallel and parallel beam and target polarizations, oriented longitudinally L and transverse T to the beam direction. Transmission measurements of the $\Delta\sigma_L(np)$ and $\Delta\sigma_T(np)$ energy dependences over 1.2–3.7 GeV have been proposed [1,2] and started [3,4,5] in Dubna. The main aim of this experimental program is to extend studies of the fundamental nucleon-nucleon (NN) interaction over a new highest energy region of free polarized neutron beams.

To implement the proposed $\Delta\sigma_{L,T}(np)$ experimental program, a large Argonne-Saclay polarized proton target (PPT) was reconstructed in Dubna [6,7], and a new polarized neutron beam line with suitable parameters was constructed and tested [8,9]. A set of necessary neutron detectors with corresponding electronics, an enough modern data acquisition system [10] and other needed equipment were also prepared, tuned and tested. Early in 1995, first three $\Delta\sigma_L(np)$ data points were successfully measured at neutron beam energies of 1.19, 2.49, and 3.65 GeV [3,4,5].

A new PPT polarizing solenoid [11] was constructed and tested at the JINR LHE for the purpose of continuing the $\Delta\sigma_{L,T}(np)$ measurements. In 1997, the presented values of $\Delta\sigma_L(np)$ were measured at 1.79 and 2.20 GeV using four combinations of two opposite polarization directions for both the beam and the target. Only one target polarization direction was available at 1.59 GeV. The preliminary results of this run were reported [12].

The NN total cross section differences $\Delta\sigma_L$ and $\Delta\sigma_T$ together with the spin-independent total cross section $\sigma_{0\mathrm{tot}}$ are linearly related to three nonvanishing imaginary parts of the NN forward scattering amplitudes via optical theorems. They are used for absolute normalization in any theoretical or phenomenological analysis. The $\Delta\sigma_{L,T}$ data check predictions of available dynamic models of strong interactions and provide an important contribution to a database of phase-shift analyses (PSA).

The observables $\sigma_{0\mathrm{tot}}$ in pp and np interactions have been measured in the last fifty years over a very large energy region. The np spin-dependent total cross section data are rare for lack of polarized neutron beams. All the observables are measured in pure inclusive transmission experiments.

The $\Delta\sigma_{L,T}(np)$ data at the same energy allow a direct determination of the imaginary parts of the spin dependent np forward scattering amplitudes. It is also possible to deduce the $\Delta\sigma_{L,T}$ nucleon-nucleon isosinglet ($I = 0$) parts using the measured np quantities and the existing pp (isotriplet $I = 1$) results.

The total cross section differences for pp scattering were first measured at the ANL-ZGS and then at TRIUMF, PSI, LAMPF, and SATURNE II. The results cover an energy range from 0.2 to 12 GeV. Other data points were measured at 200 GeV at FERMILAB for pp and $\bar{p}p$ interactions [13]. Measurements with incident charged particles need a different experimental set-up than neutron-proton experiments due to the contribution of electromagnetic interactions. The existing results are discussed in review [14] and references therein.

For the first time, the $\Delta\sigma_L(pn)$ results from 0.51 to 5.1 GeV were deduced from the $\Delta\sigma_L(pd)$ and $\Delta\sigma_L(pp)$ measurement at the ANL-ZGS in 1981 [15]. Taking a simple difference between the pd and pp results, corrected only for Coulomb-nuclear rescattering and

deuteron break-up, yields data in qualitative agreement with free np results. The correction for Glauber-type rescattering including 3-body state final interactions [16] provides a disagreement [14]. For these reasons, the ANL-ZGS pn results were omitted in the majority of existing PSA solutions.

The $\Delta\sigma_T$ and $\Delta\sigma_L$ results using free polarized neutrons, were first obtained at SATURNE II in 1987. These measurements yielded four points with relatively large errors [17]. These results have been completed by new accurate measurements at 9 to 10 energies, between 0.31 and 1.10 GeV for each observable [18,19]. The Saclay results were soon followed by PSI measurements [20] at 7 energy bins from 0.180 to 0.537 GeV using a continuous neutron energy spectrum. The PSI and Saclay sets allowed one to deduce the imaginary parts of np and $I = 0$ spin-dependent forward scattering amplitudes.[14,19].

The $\Delta\sigma_L(np)$ was also measured at five energies between 0.484 and 0.788 GeV at LAMPF [21]. A quasi-monoenergetic polarized neutron beam was produced in the $p + d \Rightarrow n + X$ scattering of longitudinally polarized protons. Large neutron counter hodoscopes had to be used because of a small neutron beam intensity.

At low energies, the $\Delta\sigma_L(np)$ at 66 MeV was measured at the PSI injector [22] and at 16.2 MeV in Prague [23]. The $\Delta\sigma_T(np)$ was determined at 9 energies between 3.65 and 11.6 MeV [24] in TUNL and at 16.2 MeV in Prague [25]. Recently in TUNL, the $\Delta\sigma_L(np)$ was measured at 6 energies between 4.98 and 19.7 MeV and $\Delta\sigma_T(np)$ at 3 other energies between 10.7 and 17.1 MeV. The latter results are still unpublished, and we refer to the George Washington University and Virginia Polytechnic Institute (GW/VPI) PSA database [26] (SAID SP99).

All JINR results are smoothly connected with the existing $\Delta\sigma_L(np)$ data at lower energies and show a fast decrease to zero between 1.1 and 2.0 GeV. They are compared with model predictions and the PSA fits. The values of the $I = 0$ part of $\Delta\sigma_L$ are also presented. The $\Delta\sigma_L(I = 0)$ and $\Delta\sigma_L(I = 1)$ energy dependences and hence a behaviour of spin dependent NN-amplitudes, are different over the measured energy range.

We give a brief determination of the measured observables in Section 2. Section 3 describes the method of the measurement. Essential details concerning the beams, the polarimeters, the experimental set-up and PPT are treated in Section 4. The data acquisition and analysis are described in Section 5. The results and discussion are presented in Section 6.

2. DETERMINATION OF OBSERVABLES

In this paper, we use the NN formalism and the notations for elastic nucleon-nucleon scattering observables from [27].

The general expression of the total cross section for a polarized nucleon beam transmitted through a PPT, with arbitrary directions of beam and target polarizations, $\vec{P}_B$ and $\vec{P}_T$, respectively, was first deduced in Refs. 28,29. Taking into account fundamental conservation laws, it is written in the form :

$$\sigma_{\rm tot} = \sigma_{0\rm tot} + \sigma_{1\rm tot}(\vec{P}_B, \vec{P}_T) + \sigma_{2\rm tot}(\vec{P}_B, \vec{k})(\vec{P}_T, \vec{k}), \qquad (2.1)$$

where $\vec{k}$ is a unit vector in the beam momentum direction. The term $\sigma_{0\rm tot}$ is the total cross section for unpolarized particles, and the $\sigma_{1\rm tot}$, $\sigma_{2\rm tot}$ are the spin-dependent contributions.

They are related to the measurable observables $\Delta\sigma_T$ and $\Delta\sigma_L$ by :

$$-\Delta\sigma_T = 2\sigma_{1\mathrm{tot}}, \tag{2.2}$$

$$-\Delta\sigma_L = 2(\sigma_{1\mathrm{tot}} + \sigma_{2\mathrm{tot}}), \tag{2.3}$$

called "total cross section differences". The negative signs for the $\Delta\sigma_T$ and $\Delta\sigma_L$ in Eqs.(2.2) and (2.3) correspond to a usual, although unjustified, convention in the literature. The $-\Delta\sigma_T$ and $-\Delta\sigma_L$ are measured as the differences of total nucleon-nucleon cross sections for parallel and antiparallel beam and target polarization directions. Polarization vectors are transversely oriented with respect to $\vec{k}$ for $-\Delta\sigma_T$ measurements and longitudinally oriented for $-\Delta\sigma_L$ experiments.

The total cross section differences are determined by an arbitrary pair of one parallel and one antiparallel beam and target polarization directions. For $\vec{P}_B$ and $\vec{P}_T$, both oriented along $\vec{k}$, we obtain four total cross sections :

$$\sigma(\rightrightarrows) = \sigma_{0\mathrm{tot}} + |P_B^+ P_T^+|\ (\sigma_{1\mathrm{tot}} + \sigma_{2\mathrm{tot}}), \tag{2.4a}$$

$$\sigma(\leftrightarrows) = \sigma_{0\mathrm{tot}} - |P_B^- P_T^+|\ (\sigma_{1\mathrm{tot}} + \sigma_{2\mathrm{tot}}), \tag{2.4b}$$

$$\sigma(\rightleftarrows) = \sigma_{0\mathrm{tot}} - |P_B^+ P_T^-|\ (\sigma_{1\mathrm{tot}} + \sigma_{2\mathrm{tot}}), \tag{2.4c}$$

$$\sigma(\leftleftarrows) = \sigma_{0\mathrm{tot}} + |P_B^- P_T^-|\ (\sigma_{1\mathrm{tot}} + \sigma_{2\mathrm{tot}}). \tag{2.4d}$$

In principle, an arbitrary pair of one parallel and one antiparallel beam and target polarization direction determines $\Delta\sigma_L$. Using two independent pairs, we also remove an instrumental asymmetry.

Bellow, we consider the neutron beam and the proton target. Since the $\vec{P}_B$ direction at the Synchrophasotron could be reversed every cycle of the accelerator, it is preferable to calculate $\Delta\sigma_L$ from measurements for $|P_B^+|$ and $|P_B^-|$ pairs with the same $\vec{P}_T$ orientation. The values of $|P_T^+|$ and $|P_T^-|$ are considered to be well-known as functions of time. Taking the difference of the total cross sections for the pair of $|P_B^+|$ and $|P_B^-|$, the spin-independent term drops out, and one can obtain:

$$-\Delta\sigma_L(P_T^+) = 2\ (\sigma_{1\mathrm{tot}} + \sigma_{2\mathrm{tot}})^+ = \frac{2\ [\sigma(\rightrightarrows) - \sigma(\leftrightarrows)]}{(|P_B^+| + |P_B^-|)\ |P_T^+|}, \tag{2.5a}$$

$$-\Delta\sigma_L(P_T^-) = 2(\sigma_{1\mathrm{tot}} + \sigma_{2\mathrm{tot}})^- = \frac{2\ [\sigma(\leftleftarrows) - \sigma(\rightleftarrows)]}{(|P_B^+| + |P_B^-|)\ |P_T^-|}. \tag{2.5b}$$

A left-right asymmetry, proportional to the mean value of the beam polarization

$$|P_B| = \frac{1}{2}(|P_B^+| + |P_B^-|) \tag{2.6}$$

is continuously monitored by a beam polarimeter.

The instrumental asymmetry cancels out giving the final results as a simple average

$$-\Delta\sigma_L = \frac{1}{2}[(-\Delta\sigma_L(P_T^+)) + (-\Delta\sigma_L(P_T^-))]. \tag{2.7}$$

This is discussed in detail in Section 4. The $\sigma_{0\mathrm{tot}}$, $\Delta\sigma_T$, and $\Delta\sigma_L$ are linearly related to the imaginary parts of the three independent forward scattering invariant amplitudes $a+b$, c and d via optical theorems :

$$\sigma_{0\,\mathrm{tot}} = (2\pi/K)\ \Im m\ [a(0)+b(0)], \tag{2.8}$$

$$-\Delta\sigma_T = (4\pi/K)\ \Im m\ [c(0)+d(0)], \tag{2.9}$$

$$-\Delta\sigma_L = (4\pi/K)\ \Im m\ [c(0)-d(0)], \tag{2.10}$$

where K is the CM momentum of the incident nucleon. Relations (2.9) and (2.10) allow one to extract the imaginary parts of the spin-dependent invariant amplitudes c(0) and d(0) at an angle of $\theta = 0°$ from the measured values of $\Delta\sigma_L$ and $\Delta\sigma_T$. Note that the optical theorems provide the absolute amplitudes. These amplitudes are also determined by the PSA at any scattering angle. Using a direct reconstruction of the scattering amplitudes (DRSA), the absolute amplitudes are determined at $\theta = 0°$ only, whereas one common phase remains undetermined at any other angle. The PSA and DRSA approaches are complementary phenomenological analyses, as discussed in [30,31].

Using the measured values of $\Delta\sigma(np)$ and the existing $\Delta\sigma(pp)$ data at the same energy, one can deduce $\Delta\sigma_{L,T}(I=0)$ as :

$$\Delta\sigma_{L,T}(I=0) = 2\Delta\sigma_{L,T}(np) - \Delta\sigma_{L,T}(pp). \tag{2.11}$$

3. METHOD OF MEASUREMENT

If N_{in} is the number of neutrons entering the target and N_{out} the number of neutrons transmitted by the target into solid angle Ω subtended by a transmission detector from the center of the target, then the total cross section $\sigma(\Omega)$ is related to the measured quantities:

$$N_{\mathrm{out}} = N_{\mathrm{in}} \exp[-\sigma(\Omega) n x], \tag{3.1}$$

where n is the number of target atoms per cm^3, x is the target thickness (cm) and $N_{\mathrm{out}}/N_{\mathrm{in}}$ is the transmission ratio. The extrapolation of $\sigma(\Omega)$ towards $\Omega = 0$ gives the unpolarized total cross section σ_{tot}.

The number of polarizable hydrogen atoms n_H is only important in the $\Delta\sigma_{L,T}(\Omega)$ measurements. The $\Delta\sigma_{L,T}(\Omega)$ depends also on the polarizations $P_B^{\pm}$ and $P_T^{\pm}$ as shown in Eqs.(2.5). Summing over the events taken with one fixed target polarization P_T^+ or P_T^- and using Eqs.(2.5a) or (2.5b), we can obtain a double transmission ratio corresponding to a difference of two values of $\sigma(\Omega)$ for P_B^- and P_B^+

$$R^{\pm} = \frac{(N_{\mathrm{out}}/N_{\mathrm{in}})^-}{(N_{\mathrm{out}}/N_{\mathrm{in}})^+} = \exp\ [\Delta\sigma(\Omega)\ P_B P_T^{\pm} n_H x] \tag{3.2}$$

with the average P_B from Eq.(2.6). Since the measured monitor counts M are proportional to primary neutron flux N_{in} entering the PPT and the counts of the transmission detectors T are proportional to transmitted neutron intensity N_{out}, the neutron detector efficiencies drop down in Eq.(3.2). To determine the $\Delta\sigma_{L,T}(\Omega)$, we have

$$\Delta\sigma_L(\Omega, P_T^{\pm}) = \frac{1}{P_B . P_T^{\pm} . n_H . x} ln R(P_T^{\pm}). \tag{3.3}$$

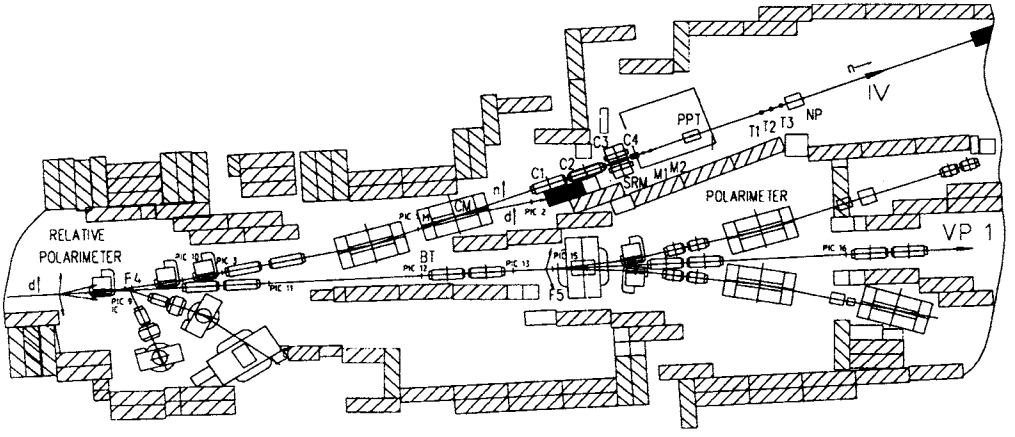

Fig. 1. Experimental set-up for the $\Delta\sigma_{L,T}(np)$ measurements. Layout of the set-up in the Experimental Hall. VP1 - beam line of extracted, polarized deuterons; 1V - beam line of polarized neutrons; BT - neutron production target; IC - ionization chamber for monitoring of deuteron beam intensity; PIC 1-3, 9-16 - multiwire proportional/ionization chambers for measurements of the deuteron beam profiles; CM - sweeping magnet; C1-C4 - set of neutron beam collimators; SRM - neutron spin rotating dipole; PPT - polarized proton target; and NP - neutron beam profilometer

We can neglect the extrapolation of $\Delta\sigma_L(\Omega)$ towards a zero solid angle ($\Omega \to 0$) due to the chosen sizes of the transmission detectors and their distances from the PPT [3,4,5]. The Saclay-Geneva (SG) PSA [31] at 1.1 GeV shows that the resulting value of $\Delta\sigma_L$ decreases at most by 0.04 mb for the angles covered by our detectors. This possible error seems to decrease with increasing energy as the PSA calculations at 1.0 GeV have shown.

The ratio of n_H to other target nuclei depends on the target material. The presence of carbon in the PPT beads adds the terms $\sigma_{\rm tot}(C)$ in Eqs.(2.4). These terms are spin-independent, and their contribution drops out in differences (2.5). The same occurs for ^{16}O and ^4He in the target. However, there are small contributions from ^{13}C and ^3He, which may be slightly polarized. This contribution was estimated to be $\pm$ 0.3 %. Uncertainties in the determination of P_B, P_T and $n_H.x$ are discussed in Section 4.

4. EXPERIMENTAL SET-UP

The experimental set-up (see Figs.1,2) for the $\Delta\sigma_{L,T}(np)$ measurements is described in [3,4,5]. We mention here only essential items important for the data analysis and results, as well as modifications and improvements of the apparatus and experimental conditions.

Both polarized deuteron and polarized free neutron beam lines [8,9], the two polarimeters [32,33], the neutron production target BT, collimators C1-C4, the spin rotation magnet SRM, the polarized proton target PPT [6,7,34], neutron beam monitors M1, M2, transmission detectors T1-T3 and the apparatus for monitoring the neutron beam profiles NP are shown in Figs.1,2. The associated electronics and the data acquisition system are also described in [3,4,5,10].

Deuterons were extracted at energies of 3.20, 3.60, and 4.40 GeV for the $\Delta\sigma_L(np)$ measurements, as well as at 1.60 GeV for the polarimetry purposes. The beam momenta p_d

were known with a relative accuracy of $\sim \pm 1$ %. The intensity of the primary polarized deuteron beam increased by a factor of ~ 3 to 4 with respect to the 1995 run. The average deuteron intensity over the run was $\sim 2 \times 10^9$ d/cycle. It was continuously monitored using two calibrated ionization chambers placed in the focal points F3 and F4 of the deuteron beam line before the neutron production target BT. In the 1997 run, different characteristics of the accelerated and extracted deuteron beam and the status of the used beam lines were in part available on the Laboratory Ethernet (cycle by cycle).

The beam of free quasi-monochromatic polarized neutrons was obtained by break-up of vector polarized deuterons at 0° in the BT. Neglecting the BT thickness, the laboratory momentum of neutrons $p_n = p_d/2$ with a momentum spread of FWHM $\simeq 5\%$ [35]. The BT contained 20 cm Be with a cross section of 8×8 cm^2. The passage of deuterons through air, windows and production target matter provided a deuteron beam energy decrease by 20 MeV in the BT centre, and the mean neutron energy decreased by 10 MeV [4]. The energies and laboratory momenta in the BT centre are quoted for the $\Delta\sigma_L$ results and the extracted beam energies are used for the beam polarization measurements.

The dimensions and positions of iron and brass collimators C1-C4 (Fig. 1) were the same as those described in [3,4,5]. An accurate measurement of the collimated neutron beam profiles was made in a dedicated run using nuclear photoemulsions. During the data acquisition, the position and X-,Y-profiles of the neutron beam were continuously monitored by a neutron profilometer NP with multiwire proportional chambers closely placed downstream the last transmission detector (see Figs.1,2).

The value and direction of proton beam polarization $\vec{P}_B(p)$ after deuteron break-up at 0° and for $p_p = p_d/2$ are the same as the vector polarization $\vec{P}_B(d)$ of the incident deuteron beam [36,37]. Assuming identical break-up conditions for neutrons, we have $\vec{P}_B(n) \simeq \vec{P}_B(p) \simeq \vec{P}_B(d)$. Then, one can measure $P_B(d)$ in order to know $P_B(n)$. During the run, the polarization $P_B(d)$ and hence the neutron beam polarization $P_B(n)$ were reversed every cycle, as requested.

The prepared neutron beam has the same vertical orientation of $P_B(n)$ as the accelerated and extracted deuteron beam. Such a neutron beam is suitable for the $\Delta\sigma_T(np)$ measurements. For the purpose of the $\Delta\sigma_L(np)$ measurements, we have to turn the neutron spins from the vertical to the longitudinal direction. This was done by the spin-rotating magnet SRM in the neutron beam line (Figs.1,2). The SRM magnetic field was continuously monitored by a Hall probe. The SRM setting and inhomogeneity of the magnetic field integral within the neutron beam tube can provide an additional systematic error of ± 0.2 %.

The measurement of $P_B(d)$ was carried out by the four-arm beam line polarimeter [32]. It consists of a liquid hydrogen target, situated at focus F5 of the extracted beam line VP1 (Fig.1), and two pairs of detector arms with recoil proton detection and magnetic analysis of scattered deuterons. The polarimeter can use a high intensity of deuterons. It determined the elastic dp scattering asymmetries at the kinetic energy of incident deuterons $T_{\rm kin}(d) = 1.60$ GeV and at a square of the 4-momentum transfer $t = -0.15({\rm GeV}/c)^2$. At this value of $T_{\rm kin}(d)$, the analyzing powers of this reaction are well known [38], and the chosen t-value is close to the maximum values of the analyzing powers. In principle, the $P_B(d)$ needs to be determined at one energy only since no depolarizing resonance exists [32]. On the other hand, the measurement requires to change the deuteron energy and to extract the beam in another beam line, what is a time-consuming operation. This polarimeter was used only

once before data acquisition and gave an average $|P_B(d)|$ of 0.524 ± 0.010 for positive and negative signs of the vector polarization . The possible systematic error of this measurement was ± 0.010. The admixture of the tensor components of the deuteron beam polarization, measured simultaneously by this polarimeter, was negligible.

The value of $P_B(p)$ was continuously monitored by another four-arm beam polarimeter [33] with a small acceptance of 7.1×10^{-4} sr during the data acquisition. The deuteron beam, considered as a beam of quasi-free protons and neutrons, collided with a CH_2 target, and quasi-free protons, scattered at 14° lab., were detected in coincidence with the protons detected by recoil arms. This polarimeter measured the *pp* left-right asymmetry on hydrogen and carbon at $T_{\rm kin}(p) = T_{\rm kin}(d)/2 = 0.80$ GeV. A simultaneous measurement together with the *dp* polarimeter gave the asymmetry $\epsilon(CH_2) = 0.2572 \pm 0.0071$. Subtracting the carbon and inelastic contributions, we obtained the following *pp* asymmetry on hydrogen $\epsilon(pp) = 0.2661 \pm 0.0073$.

The *pp* analyzing power A_{oono} was taken from the energy fixed GW/VPI-PSA [26] (SP99, solution 0.800 GeV) as well as from the SG-PSA [31] (solution 0.795 GeV). The values of $A_{oono}(pp)$ at 0.80 GeV were 0.4872 ± 0.0034 for the GW/VPI-PSA and 0.4821 ± 0.0009 for the SG-PSA. A mean value of 0.4846 ± 0.0017 provided $P_B(p) = P_B(d) = 0.549 \pm 0.015$.

The weighted average of both independent results from the two polarimeters, used for the calculations of the present results, was $|P_B(d)| = 0.532 \pm 0.008$. This is in excellent agreement with the value of $|P_B(d)| = |P_B(n)| = 0.533 \pm 0.009$ measured previously with the *dp* polarimeter at $T_{\rm kin}(d) = 1.662$ GeV and used in [3,4,5].

In 1995, the *pp* polarimeter provided only $\epsilon(CH_2) = 0.246 \pm 0.016$ at 0.831 GeV. If we apply the present ratio of $\epsilon(pp)/\epsilon(CH_2) = 1.0346$, we have $\epsilon(pp) = 0.255 \pm 0.017$. The discrete energy $A_{oono}(pp)$ predictions from the GW/VPI-PSA [26] (solution 0.850 GeV) and from the SG-PSA [31] (solution 0.834 GeV) give the mean value of 0.4824 ± 0.0048. We obtain $P_B(p) = P_B(d) = 0.528 \pm 0.035$ again in agreement with the *dp* polarimeter measurement.

Note that we have used the discrete energy PSA for the *pp* analyzing power calculations. Both PSA are locally energy-dependent and describe the measured observables at their own energies. The energy dependent PSA is not an adequate tool for the polarimetry purpose since the A_{oono} fit at a given energy may be smeared by all other fitted observables over a wide energy range.

We observed that $|P_b(d)|$ decreased for the running time tm (hours) as

$$P_d(tm) = P_d(tm = 0)\ (1 - 0.00154 \cdot tm)\ . \qquad (4.1)$$

The error of the linear term is $\pm$ 0.00013. Due to an unknown effect in the ion source, this decrease was independent of beam energy and was taken into account for the results. The global relative systematic error of $|P_b(d)|$ from all sources was estimated as ± 1.7 %.

The frozen-spin polarized proton target, reconstructed to a movable device [6,7,11,34], was used. The target material was 1,2-propanediol ($C_3H_8O_2$) with a paramagnetic Cr^V impurity having a spin concentration of 1.5×10^{20} cm^{-3} [39]. The propanediol beads were loaded into the thin wall teflon container 200 mm long and 30 mm in diameter placed inside the dilution refrigerator.

The weight of the propanediol beads for the completely filled container is 94.88 g. A uniform neutron intensity distribution over the target diameter is due to the collimator sizes. The target container, covering the neutron beam, was aligned along the beam axis.

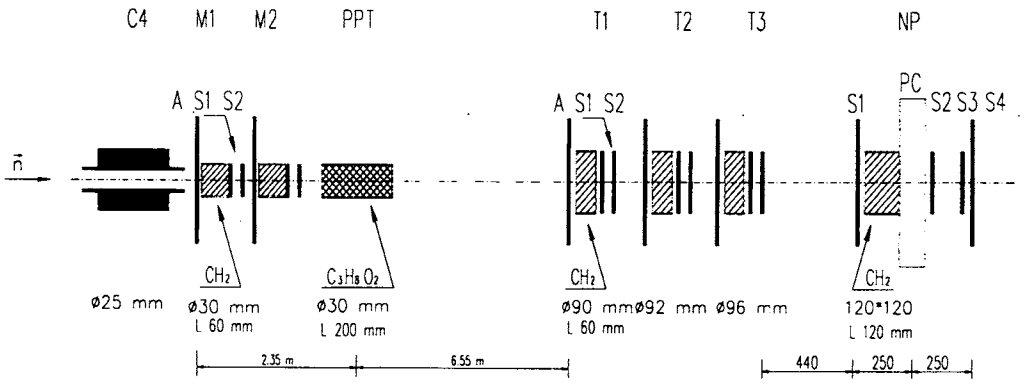

Fig. 2. Experimental set-up for the $\Delta\sigma_{L,T}(np)$ measurements. Layout of the detectors for the neutron transmission measurement. M1, M2 - monitor neutron detector modules; T1-T3 - neutron transmission detector modules; CH_2 - converters; A,S1-S4 - scintillation counters; PC - multiwire proportional chambers X,Y

In this experiment, the target was incompletely filled, and the measured weight of the beads was (73.25 $+0.80, -0.20$) g. This represents a ratio Q of 0.772 which decreases the number of hydrogen atoms per cm^2 for the target container completely filled in diameter over thickness $x' = Q \cdot x$. We have $n_H \cdot x = 8.878 \times 10^{23}/\text{cm}^2$ for full target filling and $Q \cdot n_H \cdot x = n_H \cdot x' = 6.854 \times 10^{23}/\text{cm}^2$ for the target filled over thickness x'. An additional effect on the number of hydrogen atoms per cm^2 is provided by a configuration of the beads in the target container. For the same weight of the beads, the effective number of hydrogen atoms per cm^2 is mimimal for incomplete filling with the horizontal plane of the beads. This kind of filling occured in our experiment. In this case, we have an effective value of the number of hydrogen atoms per cm^2

$$(n_H \cdot x)_{\text{eff}} = Q \cdot f \cdot n_H \cdot x = (6.405 \pm 0.19)\ 10^{23}/\text{cm}^2,$$

where the factor f includes all corrections for the configuration of propanediol beads inside the target container. The error contains uncertainties of all contributions.

The P_T measurements were carried out using a computer-controlled NMR system. The values of negative proton polarization were -0.772 at the beginning of data taking and -0.701 at the end (after 64 hours). The positive values of P_T were 0.728 and 0.710 after 34 hours, respectively. This corresponds to relaxation times of 1358 hours for P_T^+ and 663 hours for P_T^-. The relative uncertainty of the measured P_T values was estimated to be ± 5 %. This error includes uniformity measurements using the NMR data from three coils.

Neutron detector location and the associated electronics are described in [3,4,5]. The detector configuration is shown in Fig.2. The two neutron intensity monitors are denoted by M1 and M2, the three transmission detectors by T1, T2 and T3. Each detector M or T consists of a veto counter, a CH_2 radiator for a neutron produced charge-exchange reaction and two counters in coincidence. A stable power supply system was used for the photomultipliers.

The result of $\Delta\sigma_{L,T}$ is independent of neutron beam intensity if the probability of quasi-simultaneous detection of two neutrons in one transmission detector can be neglected. For

this reason, the efficiency of each detector must be relatively small, and each of the detectors must be independent of one another [4].

Dedicated tests were performed during an additional run with a high intensity unpolarized deuteron beam. Using the same transmission set-up, the neutron-carbon total cross section $\sigma_{\rm tot}(nC)$ was determined at $T_{\rm kin}(n)$ = 1.5 GeV. For this purpose, a number of carbon targets of different thicknesses were inserted in the neutron beam line instead of the PPT. The measured value of $\sigma_{\rm tot}(nC)$ agrees with the data from compilation [40].

5. DATA ANALYSIS

The following main information was recorded and displayed by the data acquisition system for each accelerator cycle:

labels of the beam polarization signs,

rates of the two calibrated ionization chambers used as primary deuteron beam intensity monitors,

rates of two neutron detectors M1 and M2 used as intensity monitors of the neutron beam incident on the PPT,

rates of three neutron transmission detectors T1, T2, and T3,

rates of the accidental coincidences for all neutron detectors M1, M2, T1, T2, T3,

rates of the left and right arms of the *pp* beam polarimeter.

Statistics at 2.2 and 1.8 GeV with P_T^- were recorded at the beginning of the run. Then, the data were taken at 2.20, 1.79 GeV, and 1.59 GeV with P_T^+. The results with P_T^- could not be obtained for the last energy.

The recorded data were then analysed in two steps. "Bad" files, as well as "empty" cycles and cycles with incorrect labels of the P_B signs, were removed in the first step. The number of "bad" cycles for the cumulated statistics represented a few tenths of a percent. The total statistics over the run obtained after the first step of the data analysis are shown in Table 1.

Since the statistics listed in one row were taken simultaneously, we see their monotonous decrease as a function of detector position. The global target transmission ratio ΣT/ΣM increases with decreasing energy.

The second step of the data analysis used the previously selected statistics in order to check the stability of the neutron detectors, to determine the parameters of the statistical distribution and to obtain the final results. The ratios of monitor and transmission detector

Table 1. Total statistics over the run for each neutron detector M1, M2, T1-T3 at different neutron beam energies and P_T signs. The count numbers for each detector are given in 10^6 units. Here, $\Sigma T/\Sigma M = 2\cdot(T1+T2+T3)/3\cdot(M1+M2)$. The energy in the BT centre is given

$T_{\rm kin}$	P_T	Statistics of detectors					$\sum T/\sum M$
(GeV)	sign	M1	M2	T1	T2	T3	
1.59	+	10.0	9.89	8.80	8.45	7.94	0.844
1.79	+	15.63	15.32	13.43	12.88	12.19	0.829
1.79	−	24.53	24.04	20.71	20.16	18.95	0.821
2.10	+	32.02	31.09	26.81	24.80	24.32	0.802
2.10	−	35.81	34.74	29.44	28.26	27.24	0.803

rates as functions of time were obtained and analysed for each neutron energy and the P_T sign. No significant time dependence of the checked values was observed.

The results were extracted using two relations (2.5a) and (2.5b). Each of them contains a hidden contribution from the instrumental asymmetry (IA) due to counter misalignments and the perpendicular components in the beam polarization. The θ and ϕ symmetries of beam neutron charge-exchange reactions in the radiators and scintillators can be strongly violated. On the other hand, the instrumental asymmetry contributions provided by the PPT are fairly negligible due to a large distance from the transmission modules. Assuming that only the measured values of $\Delta\sigma_{L,T}$ depend on the $\vec{P}_T$ direction, the $\Delta\sigma_{L,T}$ and IA effects are either added or subtracted in Eqs.(2.5a,b). For this reason, the half-sum from Eq.(2.7), i.e., a simple average, provides $\Delta\sigma_{L,T}$ whereas the half-difference gives the value of IA , as discussed in [41]. Using such a manner of obtaining the final $\Delta\sigma_{L,T}$ results, the IA contribution could be hardly suppressed.

Due to the longitudinal $\vec{P}_B$ direction and full axial symmetry, the IA is usually small for the $\Delta\sigma_L$ experiment. It can be very large for the $\Delta\sigma_T$ measurement, where no symmetry exists. One can see that the results strongly depend on the detector stabilities and their fixed positions over the data acquisition with both P_T signs. For stable detectors, a pure $\Delta\sigma_{L,T}$ effect is expected to be time-independent and equal for each transmission detector, within statistical errors. In contrast, the value of IA depends on each individual neutron detector, including the monitors.

The $-\Delta\sigma_L(np)$ values for both signs of P_T, their half differences and half-sums are listed in Table 2. All the results were obtained using common statistics from both monitors M1 and M2. Abreviation T1,2,3 signifies that the entire statistics from all the T-detectors were taken into account.

One can see that the IA was much smaller for modules T1 and T3 than for module T2. The IA values change their sign for almost all modules between 1.79 and 2.20 GeV. Since

Table 2. The measured $-\Delta\sigma_L(np)$ values at different energies in the PPT centre for the two opposite target polarizations, for individual transmission detectors and for the cumulated statistics. Instrumental asymmetry (IA) and the averaged $-\Delta\sigma_L(np)$ data are deduced. The quoted errors are statistical only

$T_{\rm kin}$ (GeV)	Transm. detectors	$-\Delta\sigma_L(P_T^+)$ (mb)	$-\Delta\sigma_L(P_T^-)$ (mb)	IA (mb)	Average $-\Delta\sigma_L$ (mb)
1.59	T1	$+4.70 \pm 3.85$			$+4.70 \pm 3.85$
	T2	$+5.45 \pm 3.90$			$+5.45 \pm 3.90$
	T3	$+1.96 \pm 3.99$			$+1.96 \pm 3.99$
	T1,2,3	$+4.07 \pm 2.85$			$+4.07 \pm 2.85$
1.79	T1	$+0.71 \pm 3.03$	$+2.52 \pm 2.29$	-0.90 ± 1.90	$+1.62 \pm 1.90$
	T2	-4.17 ± 3.07	$+0.22 \pm 2.31$	-2.20 ± 1.92	-1.97 ± 1.92
	T3	-0.93 ± 3.13	-0.28 ± 2.36	-0.32 ± 1.96	-0.60 ± 1.96
	T1,2,3	-1.45 ± 2.24	$+0.85 \pm 1.68$	-1.15 ± 1.40	-0.30 ± 1.40
2.20	T1	$+3.43 \pm 2.07$	$+2.00 \pm 1.82$	$+0.72 \pm 1.38$	$+2.71 \pm 1.38$
	T2	$+4.05 \pm 2.13$	-2.02 ± 1.85	$+3.03 \pm 1.41$	$+1.01 \pm 1.41$
	T3	-0.07 ± 2.14	$+0.35 \pm 1.88$	-0.21 ± 1.42	$+0.14 \pm 1.42$
	T1,2,3	$+2.50 \pm 1.53$	$+0.13 \pm 1.34$	$+1.19 \pm 1.02$	$+1.31 \pm 1.02$

the elements of the detectors were not moved during the run, we assume that the residual perpendicular components in $\vec{P}_B$ were opposite.

Relative normalization and systematic errors from different sources are summarized as follows:

Beam polarization including time dependence	$\pm$ 1.7 %
Target polarization	$\pm$ 5.0 %
Number of the polarizable hydrogen atoms including a filling mode	$\pm$ 1.5 %
Neutron spin rotator	$\pm$ 0.2 %
Polarization of other atoms	$\pm$ 0.3 %
Inefficiencies of veto counters	$\pm$ 0.1 %
Total of relative systematic errors	$\pm$ 5.5 %
Absolute error due to the extrapolation of the $-\Delta\sigma_L(np)$ results towards $\Omega = 0$	< 0.04 mb

6. RESULTS AND DISCUSSION

The final $-\Delta\sigma_L(np)$ values are presented in Table 3 and Fig. 3. The statistical and systematic errors are quoted. The total errors are the quadratic sums of both uncertainties. As the measurement at 1.59 GeV was carried out with one sign of P_t only, the instrumental ϕ-asymmetry could not be removed using Eq.(2.7). For this energy, we added the weighted average of the absolute IA values at 1.79 and 2.20 GeV ($\pm$ 1.18 mb) in quadrature to the overall systematic error.

The results from Refs.3,4,5 together with the existing $\Delta\sigma_L(np)$ data [17-21], obtained with free polarized neutrons at lower energies, are also shown in Fig. 3. We can see that the new results are smoothly connected with the lower energy data and confirm a fast decrease to zero within a 1.2-2.0 GeV energy region, observed previously [3,4,5].

The solid curves show the last energy-dependent GW/VPI-PSA [26] fits (SAID FX98 and SP99 solutions) of this observable over the interval from 0.1 to 1.3 GeV. Note that the present GW/VPI-PSA np database contains the JINR $\Delta\sigma_L(np)$ result at 1.2 GeV [3,4,5]. Above 1.1 GeV (SATURNE II), the np database is insufficient and a high energy part of the $\Delta\sigma_L(np)$ predictions [26] still disagrees with the measured data. Note that no extrapolation is allowed out of the region of the PSA validity. Concerning pp elastic scattering, the GW/VPI-PSA covers an energy range of up to 2.55 GeV and the SG-PSA up to 2.7 GeV. Both PSA contain almost all existing NN data. Data of the ANL-ZGS scattering experiments together

Table 3. The final $-\Delta\sigma_L(np)$ results. The total errors are quadratic sums of the statistical and systematic ones. The energy and laboratory momenta of the neutron beam correspond to the production target centre

$T_{\rm kin}$ (GeV)	$p_{\rm lab}$ (GeV/c)	$-\Delta\sigma_L(np)$ (mb)	Statis. error (mb)	System. error (mb)	Total error (mb)
1.59	2.35	+4.07	$\pm$2.85	$\pm$1.20	$\pm$3.10
1.79	2.56	−0.30	$\pm$1.40	$\pm$0.02	$\pm$1.40
2.20	2.99	+1.31	$\pm$1.02	$\pm$0.07	$\pm$1.02

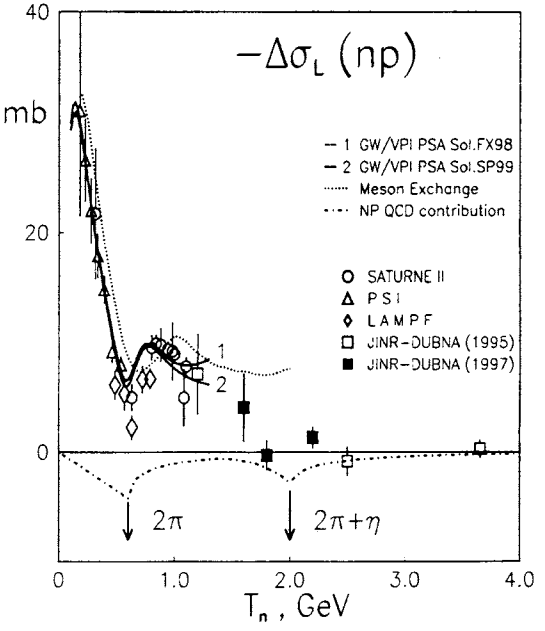

Fig. 3. Energy dependence of the $-\Delta\sigma_L(np)$ observable obtained with free neutron polarized beams. The curves are explained in the text

Table 4. The $-\Delta\sigma_L(I=0)$ values deduced from the present $\Delta\sigma_L(np)$ results and existing $\Delta\sigma_L(pp)$ data. The energies of $\Delta\sigma_L(pp)$ data and corresponding references are also listed

$T_{\rm kin}(np)$ (GeV)	$T_{\rm kin}(pp)$ (GeV)	$-\Delta\sigma_L(pp)$ (mb)	Ref. pp	$-\Delta\sigma_L(I=0)$ (mb)
1.59	1.594	$+4.93 \pm 0.30$	[47]	$+3.2 \pm 6.2$
1.79	1.798	$+3.39 \pm 0.10$	[47]	-4.0 ± 2.8
2.20	2.176	$+2.28 \pm 0.10$	[43]	$+0.3 \pm 2.0$

with the $\Delta\sigma_L(pp)$ results [42,43,44] allowed one to perform the fixed energy PSA at 6 and 12 GeV/c [45,46].

Using Eq.(2.12), one can deduce the values of $\Delta\sigma_L(I=0)$ from the obtained $\Delta\sigma_L(np)$ results and the existing $\Delta\sigma_L(pp)$ data. For this purpose, we used the ANL-ZGS [43] and SATURNE II [47] $\Delta\sigma_L(pp)$ data. The results are given in Table 4 and in Fig. 4. Since the pp data are accurate, the values of $-\Delta\sigma_L(I=0)$ have roughly two times larger errors than the obtained np results. For this reason, an improved accuracy of np measurements is important.

The values of $-\Delta\sigma_L(I=0)$ from [3,4,5] together with the ones using the $\Delta\sigma_L(np)$ data sets [17-21] are also plotted in Fig. 4. All the results are compatible and suggest a shoulder or a maximum over a region of 1.2-1.6 GeV followed by a rapid decrease with increasing energy. The solid curves represent the recent GW/VPI-PSA [26] (SAID FX98 and SP99) energy-dependent predictions for $-\Delta\sigma_L(I=0)$. In addition, the $-\Delta\sigma_L(I=1)$ fit SAID SP99 is also shown. It should be noted that the $\Delta\sigma_L(pp)$ data set is richer in the energy

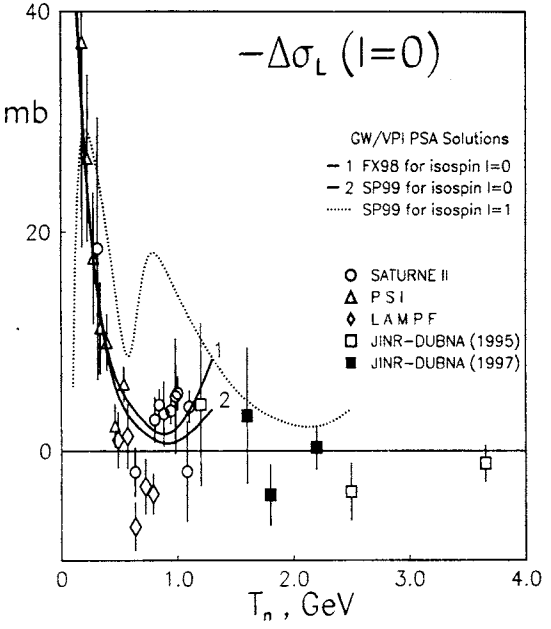

Fig. 4. Energy dependence of the $-\Delta\sigma_L(I=0)$. The notation is the same as in Fig.3

region of interest and the continuation of the $\Delta\sigma_L(np)$ measurements in Dubna is highly desirable to obtain the $\Delta\sigma_L(I=0)$ quantities at energies corresponding to the pp data.

A number of dynamic models have predicted the $\Delta\sigma_{L,T}$ energy behaviour for np and pp interactions. Below 2.0 GeV, a usual meson exchange theory of NN scattering [48] gives the $\Delta\sigma_L(np)$ energy dependence as shown by the dotted curve in Fig. 3. It can be seen that this model provides a qualitative description only.

Another dynamic model prediction for the $\Delta\sigma_L(np)$ energy dependence was discussed in [3,4,5]. This prediction concerns a contribution to the $\Delta\sigma_L(np)$ value from nonperturbative flavour-dependent interaction between quarks, induced by a strong fluctuation of vacuum gluon fields, i.e., instantons (see, for example [49,50,51]). An anomalous energy dependence of the instanton-induced interaction near 2π and $2\pi+\eta$ thresholds leads to large contributions of this mechanism to spin-dependent cross sections. A qualitatively estimated contribution of the instanton-induced interaction to the $\Delta\sigma_L(np)$ energy dependence is shown in Fig.3 by a dashed line.

The investigated energy region corresponds to a possible generation of heavy dibaryons with masses $M > 2.4$ GeV (see review [52]). For example, the model [53,54] predicts the formation of a heavy dibaryon state with a colour octet-octet structure.

A possible manifestation of exotic dibaryons in the energy dependence of different pp and np observables was predicted by another model [55-59]. The authors used the Cloudy Bag Model and R matrix to connect a long-range meson-exchange force region with a short-range region of asymptotically free quarks. The model gives the lowest lying exotic six-quark configurations in the isosinglet and spin-triplet state $^3S_1$ with M = 2.63 GeV ($T_{\rm kin}$ = 1.81 GeV). The $^3S_1$ partial wave is expected to be predominant for the $I=0$ state. The measurements of the $\Delta\sigma_{L,T}$ observables for np and the determination of the $\Delta\sigma_{L,T}(I=0)$

quantities can provide a significant check for the predicted dibaryon. Since $\Delta\sigma_T$ for an arbitrary isospin state contains no uncoupled spin-triplet, a possible dibaryon resonance effect in $^3S_1$ can be less diluted. Moreover, the spin-singlet contribution vanishes in the difference of both quantities.

The three optical theorems determine the imaginary parts of the nonvanishing forward amplitudes as shown in Eqs.(2.8) to (2.10). A maximum in the $I = 0$ amplitudes or their combinations dominanted by a spin triplet, is a necessary condition for the predicted resonance. A sufficient condition can be provided by real parts. For np scattering, they can be determined by measuring observables in the experimentally accessible backward direction, as shown in [60].

The $I = 0$ spin-dependent total cross sections represent a considerable advantage for studies of possible resonances. This is in contrast with the $I = 1$ system where the lowest lying exotic six-quark configuration corresponds to the spin-singlet state $^1S_0$. This state is not dominant, and it is hard to separate it in the forward direction. Scattering data directly related with the spin-singlet amplitude at other angles are preferable to be measured.

7. CONCLUSIONS

The new results are presented for the transmission measurements of the -$\Delta\sigma_L(np)$ energy dependence in the Dubna Synchrophasotron energy region below 3.7 GeV. The measured values of -$\Delta\sigma_L(np)$ are compatible with the existing np results, using free neutrons. A rapid decrease of the $-\Delta\sigma_L(np)$ values from 1.1 to 2.0 GeV is confirmed.

The $-\Delta\sigma_L(I = 0)$ quantities, deduced from the measured values of $-\Delta\sigma_L(np)$ and the existing $\Delta\sigma_L(pp)$ data are also presented. They indicate a shoulder or a maximum over a region of 1.2-1.6 GeV followed by a rapid decrease with energy.

The obtained results are compared with the dynamic models predictions and the recent GW/VPI-PSA fits. The necessity of further $\Delta\sigma_L(np)$ measurements and new $\Delta\sigma_T(np)$ data over a kinetic energy region above 1.1 GeV is emphasized.

ACKNOWLEDGEMENTS

The authors thank the JINR LHE and LNP Directorates for their support of these investigations. Discussions with V.N.Penev have solved several problems. We are grateful to J.Ball, M.P.Rekalo and I.I.Strakovsky for helpful suggestions.

The measurements were possible due to the JINR Directorate Grant. The work was in part supported by the International Science Foundation and Russian Government through Grant No. JHW 100, the International Association for the Promotion of Cooperation with Scientists from the Independent States of the Former Soviet Union (INTAS) through Grant No. 93-3315, the Russian Foundation for Basic Research through Grants RFBR-93-02-03961, RFBR-93-02-16715, RFBR-95-02-05807, RFBR-96-02-18736 and the Fundamental Nuclear Physics Foundation Grant 122.03.

References

1. Ball J. et al. — In: Proc.Int.Workshop "Dubna Deuteron-91", JINR, E2-92-25, Dubna, 1992, p.12.

2. Cherhykh E. et al. — In: Proc. Int. Workshop "Dubna Deuteron-93", JINR, E2-94-95, Dubna, 1994, p.185;
Proc. "V Workshop on High Energy Spin Physics", Protvino, 20-24 September 1993, Protvino, 1994, p.478.

3. Averichev S.A. et al. — In: Proc.of "VI Workshop on Spin Phenomena in High Energy Physics", Protvino, September 18-23, 1995, Protvino, 1996, v.2, p.63.

4. Adiasevich B.P. et al. — Zeitschrift für Physik, 1996, C71, p.65.

5. Sharov V.I. et al. — JINR Rapid Communications, 1996, No.3[77]-96, p.13.

6. Lehar F. et al. — Nucl. Instrum. Methods, 1995, v.A356, p.58.

7. Bazhanov N.A. et al. — Nucl. Instrum. Methods, 1996, v.A372, p.349.

8. Issinsky I.B. et al. — Acta Physica Polonica, 1994, v.B25, p.673.

9. Kirillov A. et al. — JINR Preprint E13-96-210, Dubna, 1996.

10. Chernykh E.V., Zaporozhets S.A. — Proceedings of the ESONE International Conference "RTD 94". Editors R.Pose, P.U. ten Kate, E.W.A.Lingeman; JINR Preprint E10,11-95-387, Dubna, 1995, p.179.

11. Anischenko N.G. et al. — JINR Rapid Communications, 1998, No.6[92]-98, p.49.

12. Sharov V.I. et al. — In: "Proceedings of VII Workshop on High Energy Spin Physics. SPIN-97.", July 7-12, 1997, Dubna, Russia. Editted by Efremov A.V., Selyugin O.V. JINR, E2-97-413, Dubna 1997, p.263.

13. Grosnick D.P. et al. — Phys. Rev., 1997, v.D55, p.1159.

14. Lechanoine-Leluc C., Lehar F. — Rev. Mod. Phys., 1993, v.65, p.47.

15. Auer I.P. — Phys. Rev. Lett., 1981, v.46, p.1177.

16. Grein W., Kroll P. — Nucl. Phys., 1982, v.A377, p.505.

17. Lehar F. et al. — Phys. Lett., 1987, v.189B, p.241.

18. Fontaine J.-M. et al. — Nucl. Phys., 1991, v.B358, p.297.

19. Ball J. et al. — Zeitschrift für Physik, 1994, v.C61, p.53.

20. Binz R. et al. — Nucl. Phys., 1991, v.A533, p.601.

21. Beddo M. et al. — Phys. Lett., 1991, v.258B, p.24.

22. Haffter P. et al. — Nucl. Phys., 1992, v.A548, p.29.

23. Brož J. — Zeitschrift für Physik, 1997, v.A359, p.23.

24. Wilburn W.S. et al. — Phys. Rev., 1995, v.C52, p.2353.

25. Brož J. et al. — Zeitschrift für Physik, 1997, v.A355, p.401.

26. Arndt R.A. et al. — Phys. Rev., 1997, v.C56, p.3005.

27. Bystrický J., Lehar F.,Winternitz P. — J.Physique (Paris), 1978, v.39, p.1.

28. Bilenky S.M., Ryndin R.M. — Phys. Lett., 1963, v.6, p.217.

29. Phillips R.J.N. — Nucl. Phys., 1963, v.43, p.413.

30. Ball J. et al. — Nuovo Cimento, 1998, v.A111, p.13.

31. Bystrický J., Lechanoine-LeLuc C., Lehar F. — Eur. Phys.J., 1998, v.C4, p.607.

32. Ableev V.G. et al. — Nucl. Instrum. Methods, 1991, v.A306, p.73.

33. Azhgirey L.S. et al. — Pribory i Tekhnika Experimenta, 1997, v.1 p.51; Transl. Instrum. and Exp. Techniques, 1997, v.40, p.43.

34. Bazhanov N.A. et al. — Nucl. Instrum. Methods, 1998, v.A402, p.484.

35. Ableev V.G. et al. — Nucl. Phys., 1983, v.A393, p.941 and 1983, v.A411, p.541E.

36. Cheung E. et al. — Phys. Lett., 1992, v.B284, p.210.

37. Nomofilov A.A. et al. — Phys. Lett., 1994, v.B325, p.327.

38. Ghazikhanian V. et al. — Phys. Rev., 1991, v.C43, p.1532.

39. Bunyatova E.I., Galimov R.M., Luchkina S.A. — JINR Preprint 12-82-732, Dubna, 1982.

40. Barashenkov. V.S. — *"Secheniya vzaimodeistviya chastits i yader s yadrami"*. JINR, Publishing Department, Dubna, 1993.

41. Perrot F. et al. — Nucl. Phys., 1986, v.B278, p.881.

42. Auer I.P. et al. — Phys. Lett., 1977, v.B70, p.475.

43. Auer I.P. et al. — Phys. Rev. Lett., 1978, v.41, p.354.

44. Auer I.P. et al. — Phys. Rev. Lett., 1989, v.62, p.2649.

45. Matsuda M., Suemitsu H., Watari W., Yonezawa M. — Prog. Theor. Phys., 1979, v62, 1436; 1980, v.64, 1344; 1981, v.66, p.1102.

46. Matsuda M., Suemitsu H., Yonezawa M. — Phys. Rev., 1986, v.D33, p.2563.

47. Bystrický J. et al. — Phys.Lett., 1984, v.142B, p.130.

48. Lee T.-S.H. — Phys. Rev., 1984, v.C29, p.195.

49. 't Hooft G. — Phys. Rev., 1976, v.D14, p.32.

50. Dorokhov A.E., Kochelev N.I., Zubov Yu.A. — Int. J. Mod. Phys., 1993, v.A8, p.603.

51. Dorokhov A.E., N.I.Kochelev — Sov. J. Part. Nucl., 1995, v.26, p.5.

52. Strakovsky I.I. — Fiz. Elem. Chastits At. Yadra, 1991, v.22, p.615; Transl. Sov. J. Part. Nucl., 1991, v.22, p.296.

53. Kopeliovich B.Z., Niedermayer F. — Zh. Eksp. Teor. Fiz., 1984, v.87, p.1121; Transl. Sov. Phys. JETP, 1984, v.60 (4), p.640.

54. Kopeliovich B.Z. — Fiz. Elem.Chastits At. Yadra, 1990, v.21, p.117; Transl. Sov. J. Part. Nucl., 1990, v.21 (1), p.49.

55. LaFrance P., Lomon E.L. — Phys. Rev., 1986, v.D34, p.1341.

56. Gonzales P., LaFrance P., Lomon E.L. — Phys. Rev., 1987, v.D35, p.2142.

57. LaFrance P. — Can. J. Phys., 1990, v.68, p.1194.

58. Lomon E.L. — Colloque de Physique (France), 1990, v.51, p.C6-363.

59. LaFrance P., Lomon E.L. — Proceedings of the International Conference "Mesons and Nuclei at Intermediate Energies", Dubna, 3-7 May 1994. Editors: Khankhasaev M.Kh. and Kurmanov Zh.B. World Scientific. Singapore, 1995-XV, p.97.

60. Ball J. — Eur. Phys. J., 1998, v.C5, p.57.

Received on August 13, 1999.